

DOI: <http://doi.org/10.52716/jprs.v15i3.886>

Six-Bucket Sim-Savonius Hybrid Turbine: Experimental Analysis and Performance Evaluation

Ekhlas Q. A. Fath Ali¹, Salwan O. W. Khafaji², Dhirgham Al Khafaji²

¹General Company for Communications and Informatics, Directorate of Communications and Informatics, Babylon, Iraq.

²Mechanical Engineering Department, College of Engineering, University of Babylon, Babylon, Iraq.

*Corresponding Author E-mail: eng.salown.obaid@uobabylon.edu.iq

Received 31/12/2023, Revised 20/06/2025, Accepted 20/06/2025, Published 21/09/2025



This work is licensed under a [Creative Commons Attribution 4.0 International License](https://creativecommons.org/licenses/by/4.0/).

Abstract

The growing awareness and apprehension regarding environmental issues have led to a surge in the demand for energy alternatives that are environmentally sustainable. Wind energy is widely recognized as a prominent and environmentally sustainable sort of electricity generation on a global scale. Fossil fuel is widely recognized as a crucial energy source, the accessibility of which is progressively declining. Nevertheless, wind power is considered a sustainable and renewable energy source that can serve as an alternative or supplementary option to conventional fossil fuels. Vertical axis wind turbines are good option for deployment in urban environments because to their exceptional characteristics, aesthetic appeal, minimal noise emissions, and enhanced safety measures. In order to accomplish these aims, a series of vertical axis wind turbines featuring many blades, constructed from light material, have been developed, produced, and subjected to experimental analysis to assess their performance. The turbine blade is created in the shape of a half-cylinder blade. The SIM-Savonius hybrid wind turbine's experimental evaluation involves manipulating blade angles and locations. This study investigates performance of the turbine at various speeds of winds and radius dimensions for the traditional turbine and (40cm, 50cm, 55cm) for the hybrid turbine. A graphical link was constructed between the power coefficient, blade angles, and tip speed ratio. Speed of wind, blade placement, blade count, and blade angle are all proven to have a major impact on wind turbine performance. The hybrid turbine has the highest power coefficient (31.111%) when the speed of the wind is 1.5 m/s, R is 50 cm, and r is 30 cm, the tip speed ratio (TSR) is 2.8, the blade angle is 45°. It should also be noted that the power factor of the multi-blade hybrid turbine increases by 1.383% when compared to the vertical axis wind turbine with six blades.

Keywords: Hybrid wind turbine, blade angle power coefficient, blade location, tip speed ratio.

التوربين الهجين سداسي الدلاء من نوع Sim-Savonius: التحليل التجريبي وتقييم الأداء

الخلاصة

تزايدت المخاوف البيئية وزاد الطلب على الخيارات الطاقوية المفضلة للبيئة. عالمياً، تعتبر طاقة الرياح واحدة من المصادر الخضراء المتجددة والنقية للكهرباء. الوقود الأحفوري هو واحد من أكثر مصادر الطاقة ضرورة، ويتضاءل توافره. ومع ذلك، تعتبر طاقة الرياح مصدراً للطاقة المتجددة يمكن استخدامها كبديل للوقود الأحفوري. ويعتبر الاستفادة من توربينات الرياح لإنتاج الطاقة من الرياح مناسباً للاستخدام في المواقع المبنية بسبب ميزاتها المتميزة، وجاذبيتها، وانخفاض الضوضاء، والأمان. ولتحقيق هذه الأهداف، تم تصميم توربينات الرياح ذات المحور الرأسي مع عدة شفرات (تتكون الشفرات من مادة خفيفة الوزن تم تصنيعها ودراستها تجريبياً للتحقق من أدائها). تكون شفرة التوربين على شكل نصف أسطوانية، تم تثبيتها عند زوايا ومواقع مختلفة، واختبارها عند سرعات رياح مختلفة وانصاف اقطار مختلفة للتوربين التقليدي والهجين. تم إنشاء العلاقة الرسومية بين عامل القدرة ونسبة سرعة النهاية أو الطرف. تم ملاحظة أن أداء توربينات الرياح يعتمد بشكل كبير على سرعة الهواء، موقع الشفرات وعددها وزاويتها. وان أقصى قيمة لمعامل الطاقة للتوربين الهجين تصل إلى 31.111% عندما يكون نصف القطر الكبير والصغير مساوي لـ 50 سم و 30 سم على التوالي، عندما تكون سرعة الرياح مساوي 1.5 م/ث، وخاصة عندما تكون نسبة السرعة الطرفية 2.8 وزاوية الشفرة 45 درجة. بالإضافة إلى ذلك، وجد بان مقدار الزيادة المئوية للتوربين الهجين مقارنة بالتوربين الاعتيادي وصلت إلى 1.383 بالمئة.

1. Introduction

In the present era, there exists a global competition among nations to secure energy supplies that are devoid of emissions, with the aim of safeguarding the integrity of the natural environment. Renewable wind power has exhibited significant technological advancements in recent decades, rendering it a highly viable energy supply. Wind technology plays a crucial role in addressing the issue of climate change resulting from emissions, as it lacks any radioactive or toxic components and does not generate thermal pollution. Furthermore, the efficient utilization of wind energy resources serves to mitigate environmental consequences [1]. Reference [2] introduced a methodology for the revitalization of wind farms with the objective of mitigating carbon dioxide (CO₂) emissions. Furthermore, in [2] employed multiple linear regressions to forecast speed of wind by considering many input variables, such as ambient temperature, and detectable water. Wind energy has the potential to boost the energy services reliability in regions that frequently experience inadequate grid connectivity. Additionally, it can help to improving energy security on a global scale [2] and [3]. In study [4], conducted an investigation aimed at enhancing the performance of wind turbines with twisted-bladed by determining the ideal operational and geometrical configuration. The objective of this setup was to achieve optimal performance while also ensuring a high degree of self-starting capability. The results showed that the suggested twisted rotor configuration shown improvements in both the capability for self-starting. Moreover, according of [5], conducted a comprehensive assessment of the operational efficiency of a newly developed

VAWT that incorporates twisted blades. The results showed a noticeable enhancement in the developed design compared to the conventional ones. Reference [6] conducted experiments on a hybrid rotor configuration with the aim of enhancing its efficiency under wind conditions characterized by low and moderate speed of winds. The hybrid configuration exhibited favorable performance across a diverse set of operational situations, in contrast to the individual turbine rotors operating independently. The numerical investigation conducted by [7] and the experimental investigation conducted by [8] also studied the impacts of attachment angle and radius ratio. The findings revealed that the radius ratio has a statistically significant impact on performance of the developed turbine. The hybrid rotor outperformed the Darrieus turbine rotor in terms of efficiency, and gain 20% in power coefficient. Reference [9] studied the effect of blades number on the performance of a hybrid turbine. The simulations revealed that these factors had a significant impact on the wind turbine performance. A 2-D numerical simulation was used to study effect of different geometries of Savonius blades on a hybrid rotor performance as in [10]. The geometrical parameters tested included the blade curvature, the angle of arc, and the overlap ratio of the blades. At its peak performance, the optimum rotor increased the power coefficient by 18%. Reference [11] examined the impact of the positioning of wind turbines on the performance of a hybrid wind turbine under low speed of wind conditions. The performance of the turbine under consideration exhibited superior results compared to alternative situations. Furthermore, the power extraction for the hybrid turbine was measured at 51.2%. Reference [12], conducted an experimental work to assess hybrid wind turbines performance under various configurations. Based on the trial data, it was noted that the configuration in which the Savonius rotor was affixed at the midpoint of the Darrieus turbine had the best performance compared to all other configurations. The aforementioned configuration attained a peak power coefficient of 0.2 when the parameter λ was set at 0.86. The literature described above examines the utilization of hybrid wind rotors as a means to achieve increased starting torque. Furthermore, the integration of conventional Savonius with Darrieus blades enhances the self-initiation capability, albeit at the expense of a notable reduction in power output. In addition, the hybrid rotor performance is greatly influenced by many geometric characteristics that are contingent upon the airfoil profile.

This current investigation aims to experimentally test the performance of a small VAWT. Specifically, it examines the impact of varying the rotor radius and blade angle in relation to the wind direction. An enhanced power factor and improved performance can be achieved by

optimizing the blade angle and blade radius.

2. Method

2.1. Model of the Wind Turbine

The purpose of this work is to undertake experimental work on a six-bladed VAWT, as depicted in Figures (1) and (2).

- The rotor blades are constructed from PVC material and affixed using many lightweight tubes manufactured from aluminum.
- Each blade is affixed to the tube through the utilization of an appropriate slider mechanism, facilitating effortless movement along the tube for the purpose of altering the rotor's radius.
- The blade's shape can be described as a bucket, resembling a half-cylinder, with dimensions of 50 cm in height and 20 cm in diameter.
- A laboratory fan of a particular specification is employed to produce airflow for the purpose of conducting experimental tests on wind turbines.
- The speed of wind (V) was varied at three different levels: 1.5 m/s, 2.5 m/s, and 3 m/s, as indicated in Table (1).
- The equipment depicted in Figure (3) is employed for the purpose of measuring speed of wind.
- A tri-functional device, as depicted in Figure (4), is utilized for the measurement of voltage rotational, speed, and current.

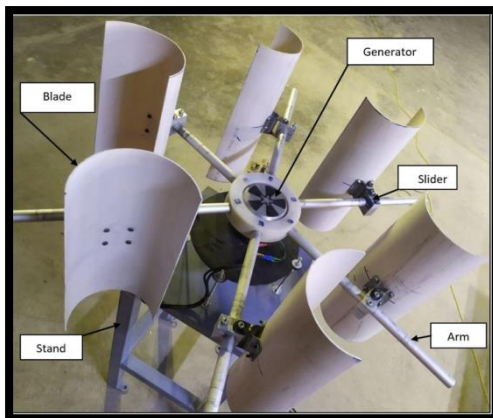


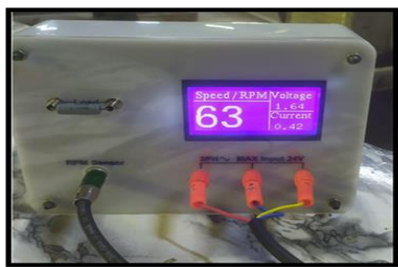
Fig. (1): Test rig of the VAWT



Fig. (2): Experimental model of MBHYVAWT.

Table (1): The VAWT Model's Geometrical Properties

Property	Symbol	Value	Unit
Blade number	N	6	–
Blade height	H	50	cm
Blade diameter	D	20	cm
Rotor radius	R	30,40,50,55	Cm
Speed of wind	V	1.5,2.5,3	m/s

**Fig. (3):** Anemometry device**Fig. (4):** Current, voltage, and rotational speed measuring unit.

2.2. Performance parameters

The provided power generated for a stream of wind (P) can be given by [13]:

$$P = \frac{1}{2} \rho_a A_T V^3 \quad (1)$$

The symbol ρ_a represents the density of air, A_T denotes the rotor projected area, and V represents the speed of wind. Nevertheless, it is important to note that no turbine is capable of fully harnessing the power generated. Therefore, the effective power generated will be influenced by the efficiency with which the energy is transported from the wind to the rotor. The metric commonly used to quantify this efficiency is referred to as the power coefficient (C_p) [14], and may be mathematically presented as follows:

$$C_p = \frac{2P_T}{\rho_a A_T V^3} \quad (2)$$

The variable P_T represents the real or observed value of the turbine power. The power coefficient is contingent upon several elements, including the rotor blade profile, blade configuration, and blade setting, among others. The designer must endeavor to establish them at their optimal level to achieve higher C_p . The propulsive force (F) can be mathematically represented as:

$$F = \frac{1}{2} \rho_a A_T V^2 \quad (3)$$

while the torque (T) generated by the rotor can be given by:

$$T = \frac{1}{2} \rho_a A_T V^2 R \quad (4)$$

The symbol R represents the rotor radius. The torque coefficient (C_T), as defined in ref. [15], is the ratio between the actual to the ideal torque. It can be mathematically expressed as follows:

$$C_T = \frac{2T_T}{\rho_a A_T V^2 R} \quad (5)$$

where T_T is the developed torque by the rotor.

The primary dimensionless metric utilized to elucidate the factors influencing the performance of the rotor is usually indicated by the tip speed ratio (TSR) or denoted as λ . It is the ratio of the speed to the velocity of wind (V), as expressed in (6) [16].

$$\lambda = \frac{R\omega}{V} = \frac{2\pi NR}{V} \quad (6)$$

In this context, the symbol ω and N are the rotor angular and rotational velocities, respectively. In the context of a specific rotor, there exists an optimal value (λ) and the power coefficient reaches its highest value ($C_p \max$). This value can be calculated by (7) as,

$$C_p = \frac{2P_T}{\rho_a A_T V^3} = \frac{2T_T \omega}{\rho_a A_T V^3} \quad (7)$$

Finally, (6) and (7) are used together to calculate the tip speed ratio, as stated in ref. [4].

$$\frac{C_p}{C_T} = \frac{R\omega}{V} = \lambda \quad (8)$$

2.3. Experimental Work

The experiment was carried out within the laboratory facilities of the University of Babylon. The testing technique can be outlined through a series of steps, which include:

- 1- The wind rotor model is positioned in alignment with a fan, wherein the fan is activated to generate varying wind velocities.
- 2- The measurement of speed of wind is conducted using an instrument known as an Anemometer, which is positioned in proximity to the rotor blade.
- 3- Two instances of VAWT were subjected to testing. The initial scenario is a VAWT with six blades, referred to as VAWTb6. The second scenario pertains to the utilization of a

multi-blade wind turbine, specifically a hybrid turbine (MBHYWT)

In this study, the turbines were tested at different speeds (1.5 m/s, 2.5 m/s, and 3 m/s) for several angles of blades included 40° , 45° , 60° , 90° , 120° , and 135° , as seen in Figure (5). The rotor radius is examined at three different values: 30 cm, 40 cm, and 50 cm. The measurement instrument previously described is utilized for measuring the rotational speed, voltage, and the output current generated by the turbine. Six blades are used. Three of them possess a constant rotor radius denoted as $r = 30$ cm, while the radial locations of the other three blades are vary by $R = 40$ cm, 50 cm, and 55 cm as shown in Figure (6).



Fig. (5): Rotor blades at different angles.

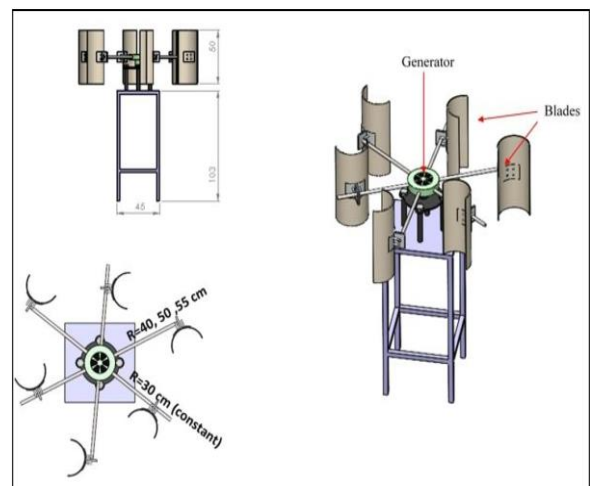


Fig. (6): Schematic of multi-blade hybrid wind turbine.

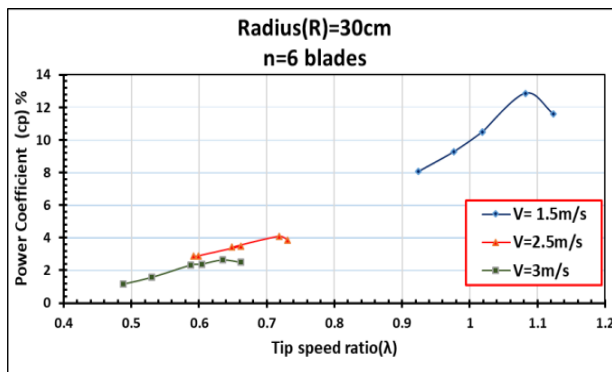
3. Results and Discussion

To assess the efficacy of power, wind rotors, and torque coefficients were acquired. Consequently, the determination of power and rotational speed (rpm) was carried out at a given speed of wind. The mathematical formulations of the dynamic torque were based on the correlation between power generation and quantifiable torque measurements. Once the data was obtained, the aforementioned mathematical formulations were utilized to ascertain the performance parameters of the rotor.

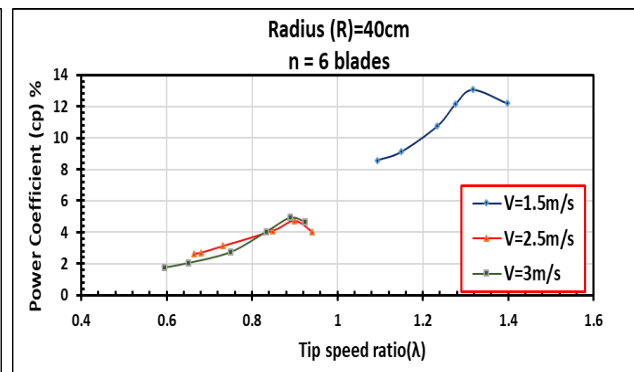
3.1. Effect of Tip Speed Ratio

Two instances of vertical axis wind turbines were subjected to testing. In the initial scenario, wherein the turbine is equipped with six blades (VAWT), the tip speed ratios and power coefficients were evaluated at three distinct wind velocities. Figure (7) illustrates the fluctuations in power coefficients resulting from changes in the tip speed ratio over various

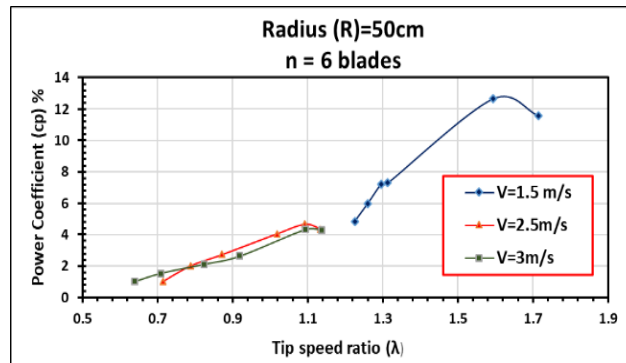
speeds of wind and radius. Figure (7-a) illustrates the power coefficients corresponding to a radius (R) of 30 cm. The primary attributes exhibited by the subfigures are to the non-linear nature of the power coefficients, which can be attributed to variations in the tip-speed ratio (TSR). In alternative terms, an observed critical value is identified for a certain wind velocity. This phenomenon is observed across various values of radius and wind velocities. Conversely, it has been shown that a turbine operating at lower tip speed ratios, which correlate to higher speed of winds, has lower power coefficients. This implies that the turbine operates in a situation known as stall mode, resulting in a decrease in the power generated by the turbine. Furthermore, it should be noted that as TSR increases, the turbine's rotational speed also increases. Nevertheless, the rapid rotation of the blades alters the aerodynamic characteristics of the surrounding airflow and induces the formation of incoming flow obstruction. This obstruction may enhance the alignment of the streamlines in order to circumvent the rotors. The primary characteristic observed in the plots depicted in Figure (7) can be traced to the opposite correlation between power coefficients and speed of wind, as indicated by (2) and (7), respectively. It is noteworthy to notice that $C_p=13.05$ when $TSR=1.3$ when the speed of wind is $V=1.5$ m/s and $R=40$ cm.



(a)



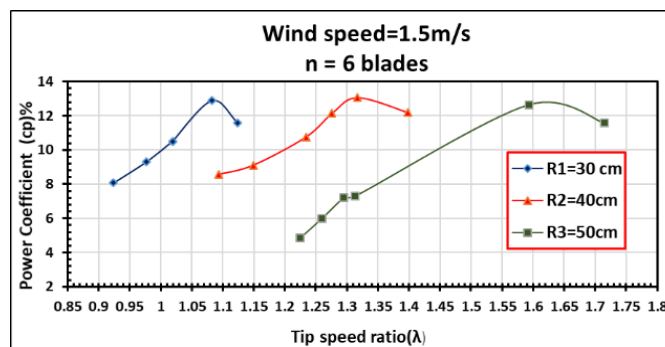
(b)



(c)

Fig. (7): Effect of blade radius and velocities on the Power coefficient.

TSR and power coefficient are depicted for varying blade locations or blade radii in Figure (8), while keeping the speed of wind constant. It is observed that the higher value of TSR is greater for the blades located at a greater distance in the design, specifically at a radius of 50 cm. This finding enhances convenience in terms of wind turbine operation. The subfigures depicted in this figure exhibit comparable behavior. However, Figure (8) demonstrates that the power coefficients reach their highest value when the speed of wind is low and the blade radius is at its maximum. In conclusion, when the rotor radius remains constant while speed of wind varies, or when the rotor radius varies while speed of wind remains unchanged, (6) demonstrates that TSR is influenced by both the radius and speed of wind. Specifically, TSR is proportional to the radius of the rotor and inversely proportional to speed of wind. As the radius increased and maintaining a constant speed of wind, the TSR increases. Conversely, as speed of wind increased and keeping the radius constant, the TSR drops.

**Fig. (8):** Effect of TSR on power coefficient.

In the second scenario, the power coefficients and TSR of the Multi-blade hybrid-vertical-axis wind turbine (MBHYWT) are evaluated for three different wind velocities. Figure (9)

illustrates the connection between the power coefficient and TSR for various rotating radii ($R = 40\text{cm}$, 50cm , and 55cm) of three blades at different angles ($\Theta = 45^\circ$, 60° , 90° , 120° , and 135°), as well as a fixed rotating radius ($r = 30\text{cm}$) for the remaining three blades of the hybrid multi-blade wind turbine. The speed of wind (V) is set at 1.5 m/s .

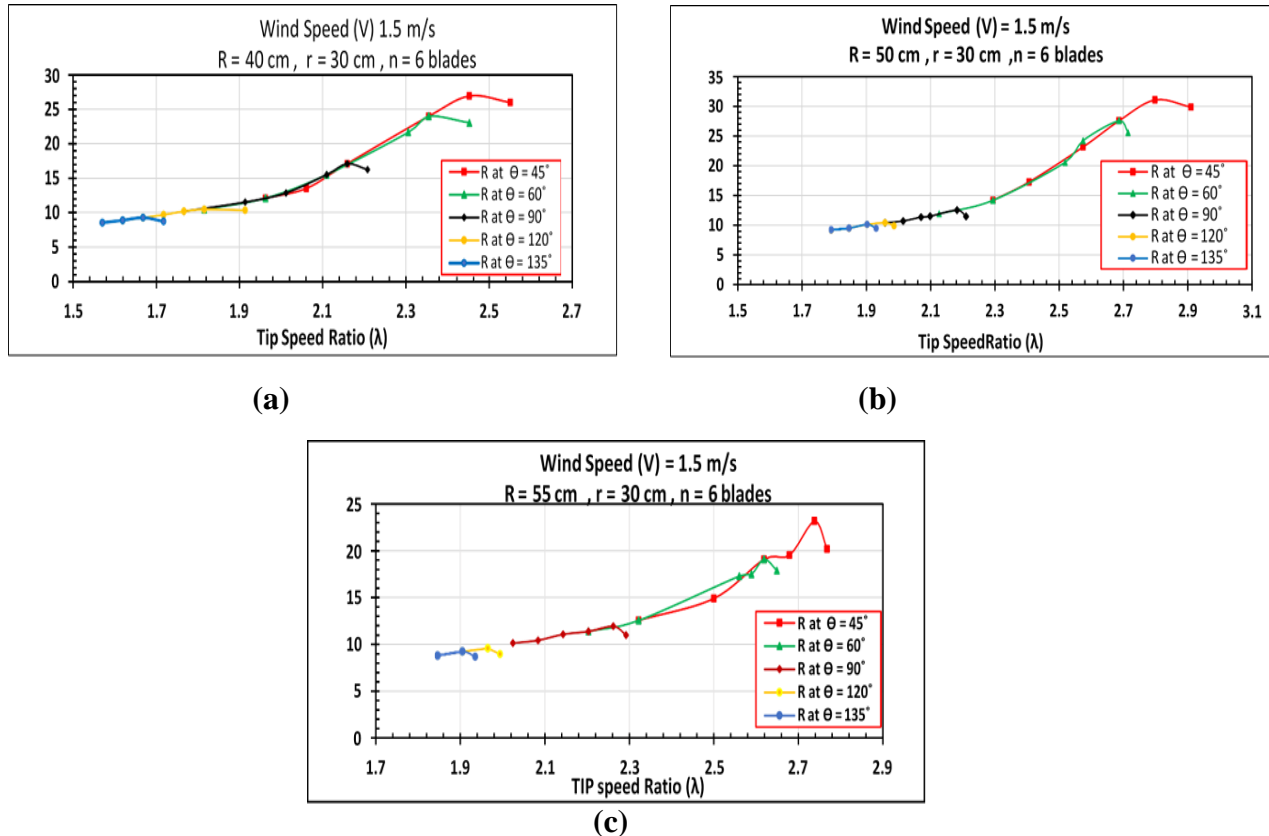


Fig. (9): Power coefficient versus TSR for different rotor radius (R) of a multi-blade hybrid wind turbine, when speed of winds (V) $= 1.5\text{ m/s}$, number of blades $= 6$.

Figure (9) demonstrates that the angle ($\Theta = 45^\circ$) corresponds the highest observed value of the power coefficient (C_p). Fig. (10) presents a comparative analysis of the greatest C_p at 1.5 m/s and 45° . The comparison is made for three different radii, namely 40 cm , 50 cm , and 55 cm . The results indicate that the highest C_p value, reaching 31.11% , is observed at a radius of 50 cm .

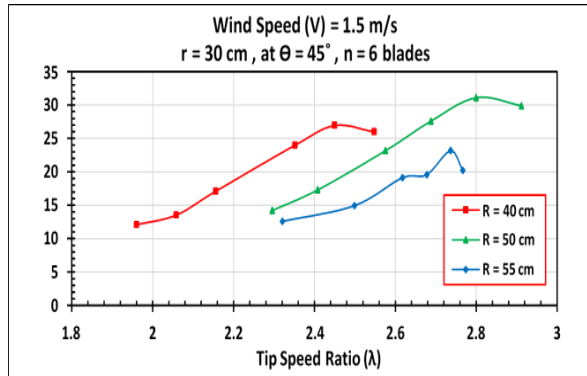


Fig. (10): Power coefficient versus TSR for R of MBHYWT

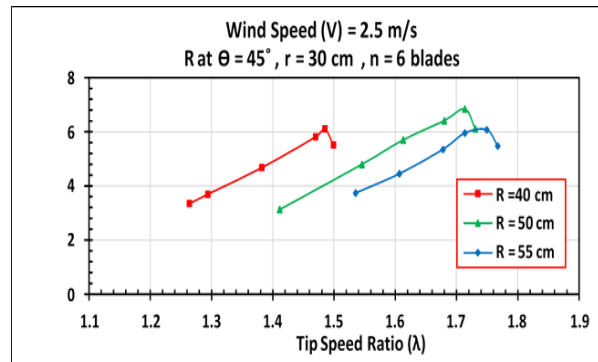


Fig. (11): Comparing power coefficient versus (TSR) for different R of MBHYWT.

Figure (11) shows a comparison of the highest value of (C_p) at ($V = 2.5$ m/s), ($R = 40$ cm, 50 cm and 55 cm) at $\Theta = 45^\circ$, so the maximum value of C_p is 6.839% at $R = 50$ cm.

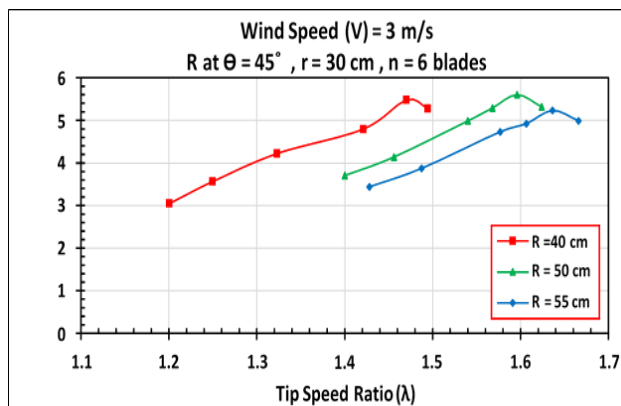


Fig. (12): Power coefficient versus TSR for different radius (R) of (MBHYWT).

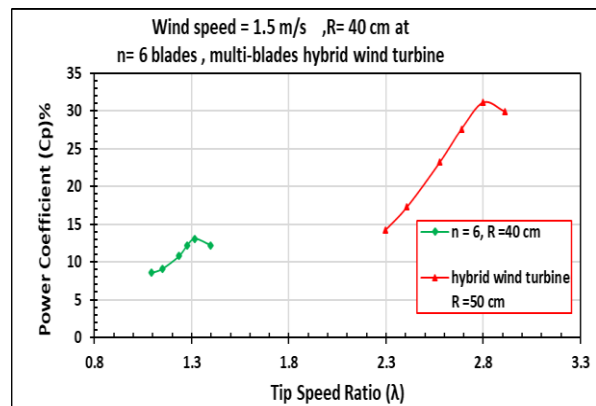


Fig. (13): Power coefficient versus TSR for different radius (R) of (MBHYWT)

Figure (12) shows a comparison of the highest value of (C_p) at ($V = 3$ m/s), ($R = 40$ cm, 50 cm and 55 cm) at $\Theta = 45^\circ$, so the maximum value of C_p is 6.606% at $R = 50$ cm, while Figure (13) shows the maximum power coefficient returns to multi-blade hybrid wind turbine (MBHYWT) compared to the six-blade turbines. Addition of another group of blades have increased the active force resulted in the generated torque and reduce effect of air stream blockage.

3.2. Effect of Blade Angle

In the initial scenario, the C_p is computed and depicted in Figure (14). It has been noticed that the maximum values, for all subfigures depicted in Figure (14), are noticed at blade angles of 45 degrees. Nevertheless, the values of these variables exhibit variation in relation to both the

speed of the wind and the blade location. The impact of blade angles becomes notable when the blade is positioned at the furthest distance from the rotational center, particularly in scenarios where speed of winds is lower, as depicted in Figure (14-c). This elucidates the relationship between power coefficients and variables like as speed of wind and blade positions, highlighting their sensitivity. Figure (15) illustrates the greatest value of C_p (13.055%) achieved at a speed of 1.5 m/s, a radius of 40 cm, and an angle of 45° .

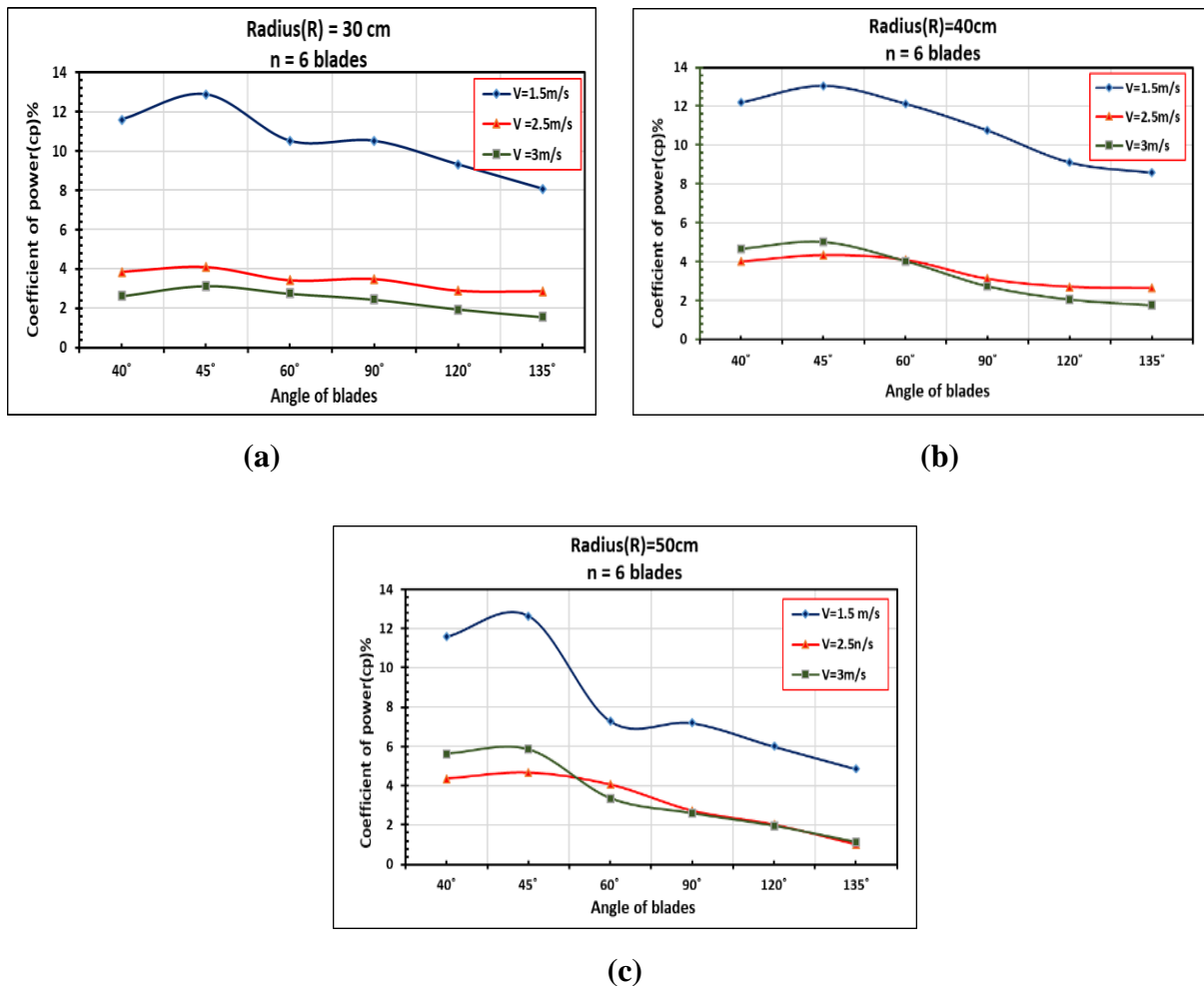


Fig. (14): Effect of rotor radius and speed of wind on the Power coefficient at different blade angles.

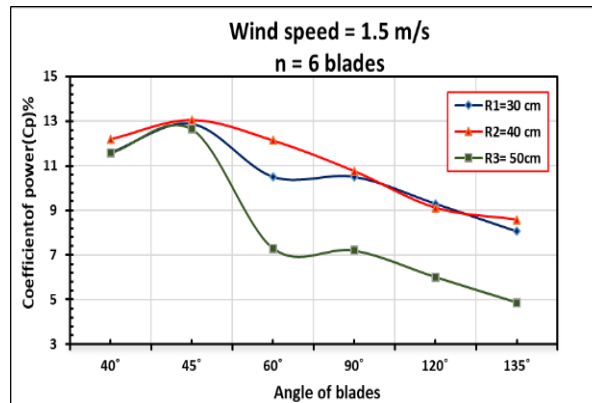


Fig. (15): Effect of blade angles on C_p for different values of rotor radius

In the second scenario using MBHYWT, the power coefficients and blade angles were determined for three speeds of wind and various rotor radii (R), as depicted in Figure (16). In this particular scenario, the highest recorded value of C_p is 31.111%.

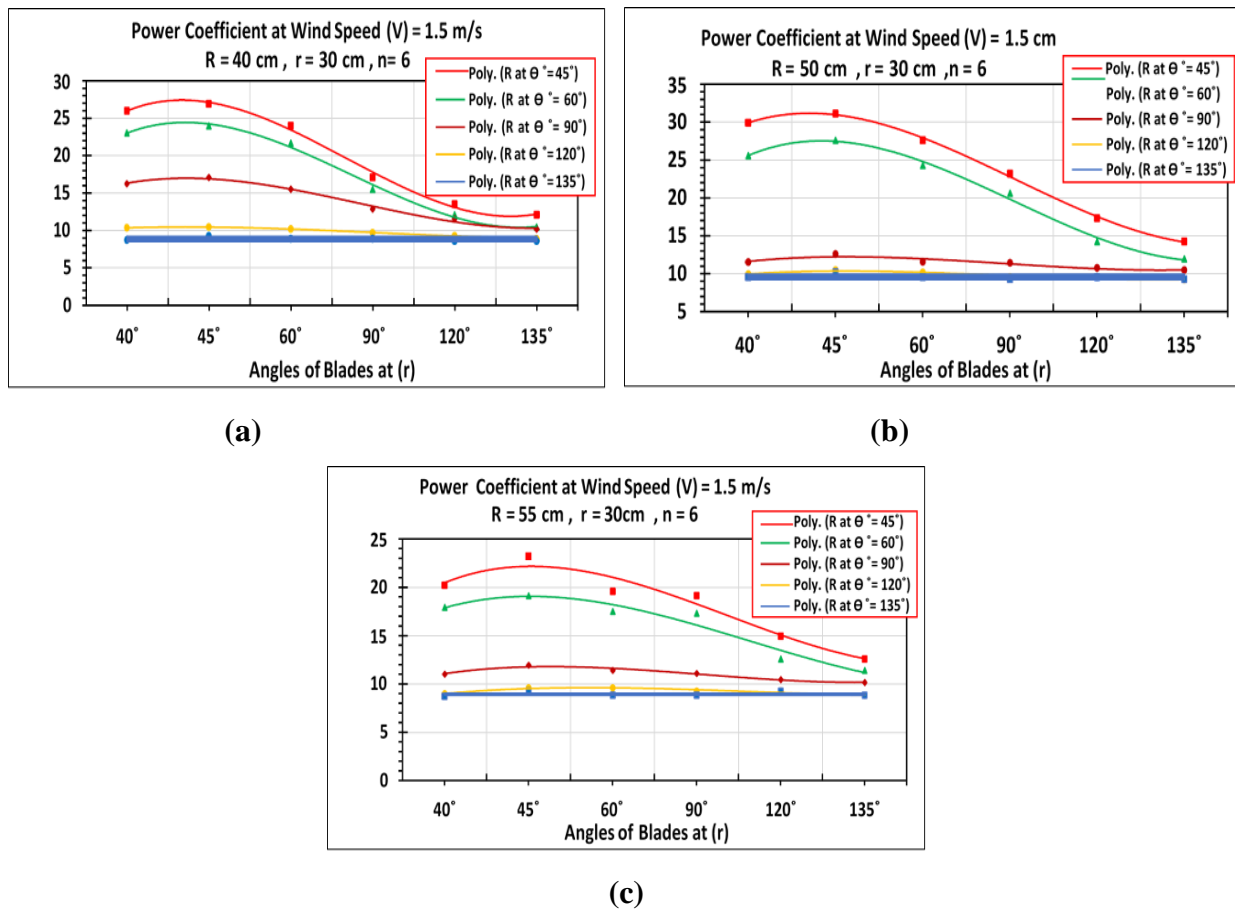


Fig. (16): Power coefficient at different blade angles of MBHYWT

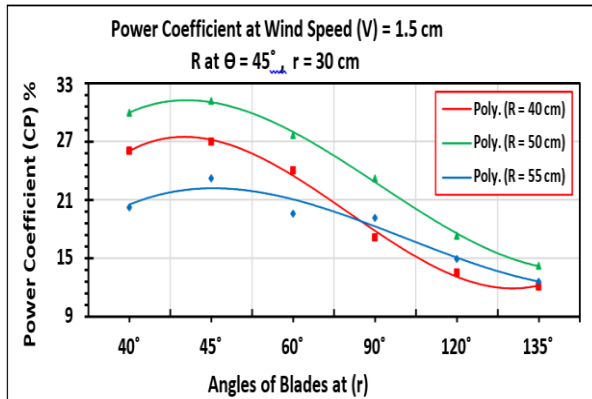


Fig. (17): Power coefficient at different blade radii and $V=1.5$ m/s.

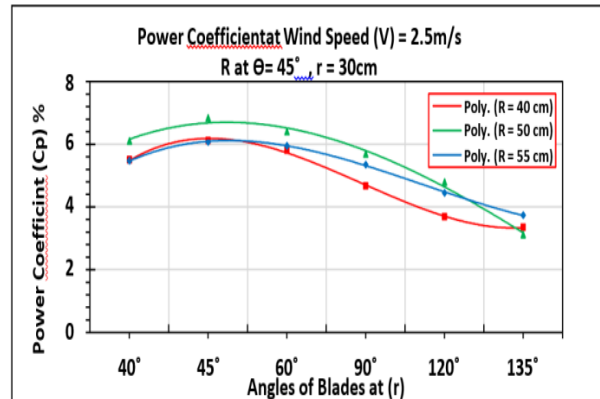


Fig. (18): Power coefficient at different blade radii and $V=2.5$ m/s.

The max. value of C_p is 6.839 % at speed of 2.5 m/s, radius of 50 cm, and angle of 45° as shown in Figure (18). While, when the speed of wind equals 3 m/s, the max. value of C_p is 6.606% at radius of 50 cm and angle of 45° as shown in Figure (19).

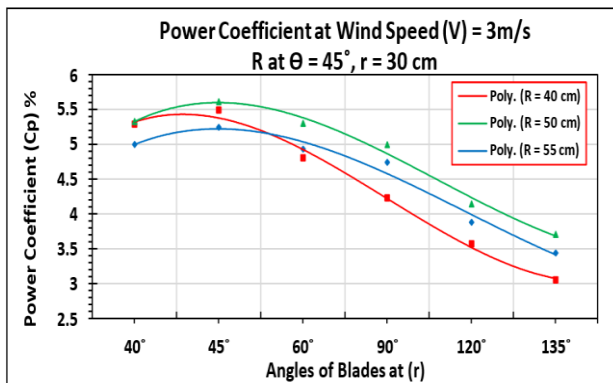


Fig. (19): Power coefficient at different blade radii.

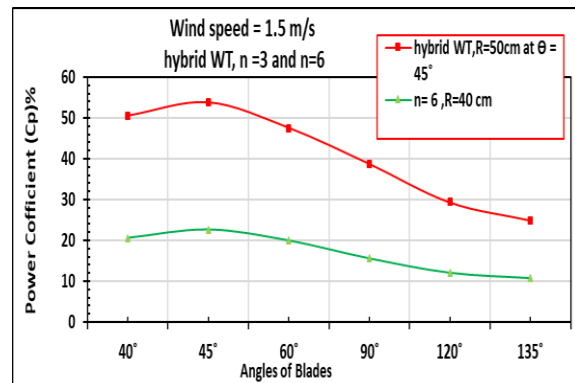


Fig. (20): Comparison between the conventional and hybrid wind turbine based on power coefficient.

Finally, to quantify the effectiveness of the proposed MBHYWT, a simple assessment is made between them at specific wind of speed and blade angles and illustrated in Figure (20). It is observed that the hybrid turbine exhibits higher power coefficient than the conventional one.

4. Conclusion

This paper presents an analysis of the fundamental concepts underpinning the technology of wind energy conversion. An investigation was conducted to analyze the impact of turbine design on the production of mechanical power under conditions of low speed of winds. The primary findings of this study are:

- 1- The performance is influenced by various factors, including speed of wind, the positioning of the blades (specifically, the rotor radius and the angle of the blades).
- 2- The hybrid turbine exhibits its highest power coefficient ($C_p = 31.111\%$) when the blade radius (R) is 50 cm, the speed of wind (r) is 30 cm, $TSR = 2.8$, blade angle ($\Theta = 45^\circ$), and the blades number ($n = 6$).
- 3- The highest values of the C_p are seen at a blade angle of 45° for all effective parameter values.
- 4- Higher power coefficients C_p can be attained by operating at lower speed of winds and utilizing larger blade radii, which in turn leads to higher tip-speed ratios (TSR).
- 5- VAWTs showed the capability to produce electrical energy suitable for local consumption, even in conditions characterized by low speed of winds.

List of symbols

Symbol	Description
VAWT	Vertical axial wind turbine
HAWT	Horizontal axial wind turbine
m	Mass
V	Velocity
E	Kinetic energy
v	volume
A_T	Projected area
ρ_a	density
P_T	Power of turbine
C_p	Power coefficient
F	Force
TSR , λ	Tip speed ratio
R	Radius of rotor

References

- [1] A. M. Abdelsalam, M. A. Kotb, K. Yousef, and I. M. Sakr, "Performance study on a modified hybrid wind turbine with twisted Savonius blades", *Energy Conversion and Management*, vol. 241, p. 114317, Aug. 2021. <https://doi.org/10.1016/j.enconman.2021.114317>.
- [2] M. Verma, "Wind farm repowering using WAsP software – an approach for reducing CO₂ emissions in the environment", *Encyclopedia of renewable and sustainable materials*, p. 844–859. 2020.
- [3] M. Verma, H. K. Ghritlahre, and G. Chandrakar, "Wind Speed Prediction of Central Region of Chhattisgarh (India) Using Artificial Neural Network and Multiple Linear Regression Technique: A Comparative Study", *Annals of Data Science*, vol. 10, pp. 851–873, 2023. <https://doi.org/10.1007/s40745-021-00332-1>.
- [4] A. S. Saad, A. Elwardany, I. I. El-Sharkawy, S. Ookawara, and M. Ahmed, "Performance evaluation of a novel vertical axis wind turbine using twisted blades in multi-stage Savonius rotors", *Energy Conversion and Management*, vol. 235, p. 114013, May 2021. <https://doi.org/10.1016/j.enconman.2021.114013>.
- [5] A. S. Saad, I. I. El-Sharkawy, S. Ookawara, and M. Ahmed, "Performance enhancement of twisted-bladed Savonius vertical axis wind turbines", *Energy Conversion and Management*, vol. 209, p. 112673, Apr. 2020. <https://doi.org/10.1016/j.enconman.2020.112673>.
- [6] A. Pallotta, D. Pietrogiaconi, and G. P. Romano, "HYBRI – A combined Savonius-Darrieus wind turbine: Performances and flow fields", *Energy*, vol. 191, p. 116433, Jan. 2020. <https://doi.org/10.1016/j.energy.2019.116433>.
- [7] G. Saini and R. P. Saini, "A numerical analysis to study the effect of radius ratio and attachment angle on hybrid hydrokinetic turbine performance", *Energy for Sustainable Development*, vol. 47, pp. 94–106, Dec. 2018. <https://doi.org/10.1016/j.esd.2018.09.005>.
- [8] K. Sahim, D. Santoso, and D. Puspitasari, "Investigations on the Effect of Radius Rotor in Combined Darrieus-Savonius Wind Turbine", *International Journal of Rotating Machinery*, 2018, p. 3568542, 2018. <https://doi.org/10.1155/2018/3568542>.
- [9] X. Liang, S. Fu, B. Ou, C. Wu, C. Y. H. Chao, and K. Pi, "A computational study of the effects of the radius ratio and attachment angle on the performance of a Darrieus-Savonius combined wind turbine", *Renewable Energy*, vol. 113, pp. 329–334, Dec. 2017. <https://doi.org/10.1016/j.renene.2017.04.071>.
- [10] A. Roshan, A. Sagharichi, and M. J. Maghrebi, "Nondimensional Parameters' Effects on Hybrid Darrieus–Savonius Wind Turbine Performance", *Journal of Energy Resources Technology*, vol. 142, no. 1, Sep. 2019. <https://doi.org/10.1115/1.4044517>.
- [11] N. M. Ali, A. A. K, and S. Aljabair, "the effect of darrieus and savonius wind turbines position on the performance of the hybrid wind turbine at low wind speed", *international journal of mechanical engineering and technology (ijmet)*, vol. 11, no. 2, Feb. 2020. <https://doi.org/10.34218/ijmet.11.2.2020.006>.
- [12] A. S. Siddiqui, S. N. Mian, M. Alam, M. S. ul Haq, A. H. Memon, and M. S. Jamil Energy, "Experimental Study to Assess the Performance of Combined Savonius Darrieus Vertical Axis Wind Turbine at Different Arrangements", *IEEE 21st International Multi-Topic Conference (INMIC)*, Karachi, Pakistan, pp. 1-8, Nov. 01, 2018. <https://doi.org/10.1109/INMIC.2018.8595538>.
- [13] M. Sathyajith, "Wind Energy: Fundamentals, Resource Analysis and Economics", *Springer*

Science & Business Media, 2006.

- [14] W. A. El-Askary, A. S. Saad, A. M. Abdelsalam, and I. M. Sakr, “Investigating the performance of a twisted modified Savonius rotor”, *Journal of Wind Engineering and Industrial Aerodynamics*, vol. 182, pp. 344–355, Nov. 2018. <https://doi.org/10.1016/j.jweia.2018.10.009>.
- [15] W. A. El-Askary, A. S. Saad, A. M. Abdelsalam, and I. M. Sakr, “Experimental and Theoretical Studies for Improving the Performance of a Modified Shape Savonius Wind Turbine”, *Journal of Energy Resources Technology-transactions of The Asme*, vol. 142, no. 12, Jun. 2020. <https://doi.org/10.1115/1.4047326>.
- [16] Y. Jiang, P. Zhao, T. Stoesser, K. Wang, and L. Zou, “Experimental and numerical investigation of twin vertical axis wind turbines with a deflector”, *Energy Conversion and Management*, vol. 209, p. 112588, Apr. 2020. <https://doi.org/10.1016/j.enconman.2020.112588>.